

Supporting information

La-doped ZnWO₄ nanorods with enhanced photocatalytic activity for NO removal: Effects of La doping and Oxygen vacancies

Junli Nie^a, Qadeer-Ul Hassan^a, Yuefa Jia^b, Jianzhi Gao^a, Jianhong Peng^a, Jiangbo Lu^a, Fuchun

Zhang^c, Gangqiang Zhu^{*,a}, Qizhao Wang^{*,b}

^aSchool of Physics and Information Technology, Shaanxi Normal University, Xi'an 710062, P.R.

China

^bSchool of Environmental Science and Engineering, Chang'an University, Xi'an 710064, P.R.

China

^cCollege of Physics and Electronic Information, Yan'an University, Yan'an 716000, P.R. China

*To whom correspondence should be addressed: Tel/Fax: +86-29-81530750

Email address: zgq2006@snnu.edu.cn, wangqizhao@163.com

1. Characterization

The XRD patterns of the samples were analyzed by a Bruker D8 Advance X-ray diffraction with Cu K α ($\lambda = 1.5418 \text{ \AA}$) radiation at a scanning speed of 6° min^{-1} . The morphologies of the samples were recorded on the FEG scanning electron microscope (FEI Nova NanoSEM 450). The elemental mapping of the samples was investigated by FEG transmission electron microscope (JEOL, JEM-2100F) attached with an energy-dispersive X-ray spectroscopy detector. The Nitrogen adsorption isotherms and Brunauer, Emmett, and Teller (BET) surface area were determined by a nitrogen adsorption apparatus (Belsorp max). Fluoromax-4 spectrophotometer (HORIBA Scientific, excited

at $\lambda = 250$ nm) was used to detect the photoluminescence spectra (PL). The UV-visible absorption spectra were recorded on the (Cary 5000, Agilent) UV-visible spectrometer in a wavelength range of 200-800 nm. The photo-electrochemical properties of the as-prepared samples were evaluated using a three-electrode system potentiostat (CHI 760D, CH Instruments, Inc.). The samples were regarded as the working electrode, 0.1 mol/L Na₂SO₄ solution was used as the electrolyte, the equipped commercial Pt plate and the saturated calomel electrode (SCE) were as the counter electrode and the reference electrode, respectively. The photocurrent density was analyzed using a 300W xenon lamp as light source (CEL-HXF300, Beijing China Education Au-light, Co. Ltd) at room temperature. XPS spectrum was carried out on a Theta Probe AR-XPS System (Thermo Fisher Scientific, Waltham, MA, USA) with monochromated Al K α X-ray source ($h\nu = 1486.6$ eV). The electron spin resonance (ESR, Bruker a300) measurement of samples were conducted by mixing the as-prepared samples in a 0.2 mL (50 mM) DMPO solution ($\cdot\text{O}_2^-$ in methanol and $\cdot\text{OH}$ in aqueous dispersion, 300W xenon lamp as light source) at room temperature.

2. Method of theoretical calculations

The first-principle calculation (DFT) was provided by Cambridge Sequential Total Energy Package (CASTEP) in the Materials Studio software. The Perdew-Burke-Ernzerhof (PBE) exchange-correlation functions were employed with a generalized gradient approximation (GGA). A plane-wave basis set with the cut-off energy at 380 eV was implemented to treat valence electrons and calculation. For the calculations of structural and electronic properties, the Brillouin zone was sampled in a 3 \times 3 \times 4 Monkhorst-pack k point grid geometry optimization. In addition, the energy of per atom was set as 5.0×10^{-6} eV, the maximum force was 0.01 eV/Å, the maximum pressure was 0.02 GPa and the maximum displacement was 5.0×10^{-4} Å.

3. Trapping experiments

In order to confirm the main function of active species, trapping experiments were conducted by using the capture agents. The capture agents including potassium dichromate ($K_2Cr_2O_7$), potassium iodide (KI), isopropanol (IPA, C_3H_8O) and the benzoquinone (PBQ) have effects on e^- , h^+ , $\cdot OH$ and $\cdot O_2^-$, respectively. Typically, 20 mg of trapping agent was mixed with 0.1 g photocatalyst, and the following process was same as the photocatalytic evaluation for the NO removal.

4. *In situ* FTIR study on photocatalytic NO oxidation process

The *in situ* FTIR equipment is composed of Tensor II FTIR spectrometer (Bruker, Germany), *in situ* reaction cell, gas system, light source and pre-treatment equipment. Firstly, the prepared sample was swept by *He* (g) (50 mL/min) for 10 min and was preheated at 200 °C for 60 min. It aims to remove the residual carbohydrates, water, and carbon dioxide that adsorbed on the surface of the photocatalyst. The FTIR spectrum after the heat treatment was utilized as the background (the background as baseline). The light source was turned on when the adsorption-desorption was completed, and the sample was illuminated for 30 min under a light source (300 W xenon lamp, CEL-HXF300, Beijing China Education Au-light, Co., Ltd). The real-time FTIR spectra were measured in the range of 600-4000 cm^{-1} to analyze the photocatalytic oxidation process of NO at 3 min time intervals.

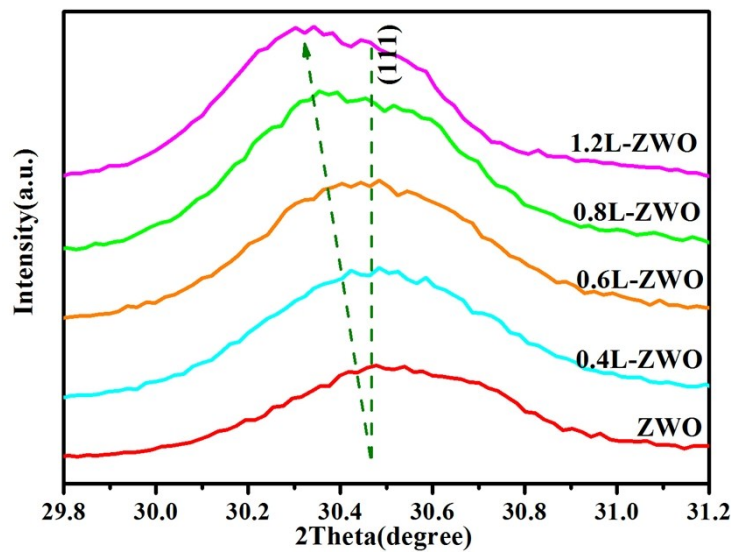


Fig. S1 The detailed XRD pattern in the range of 29.8°- 31.2° corresponding to (111) plane

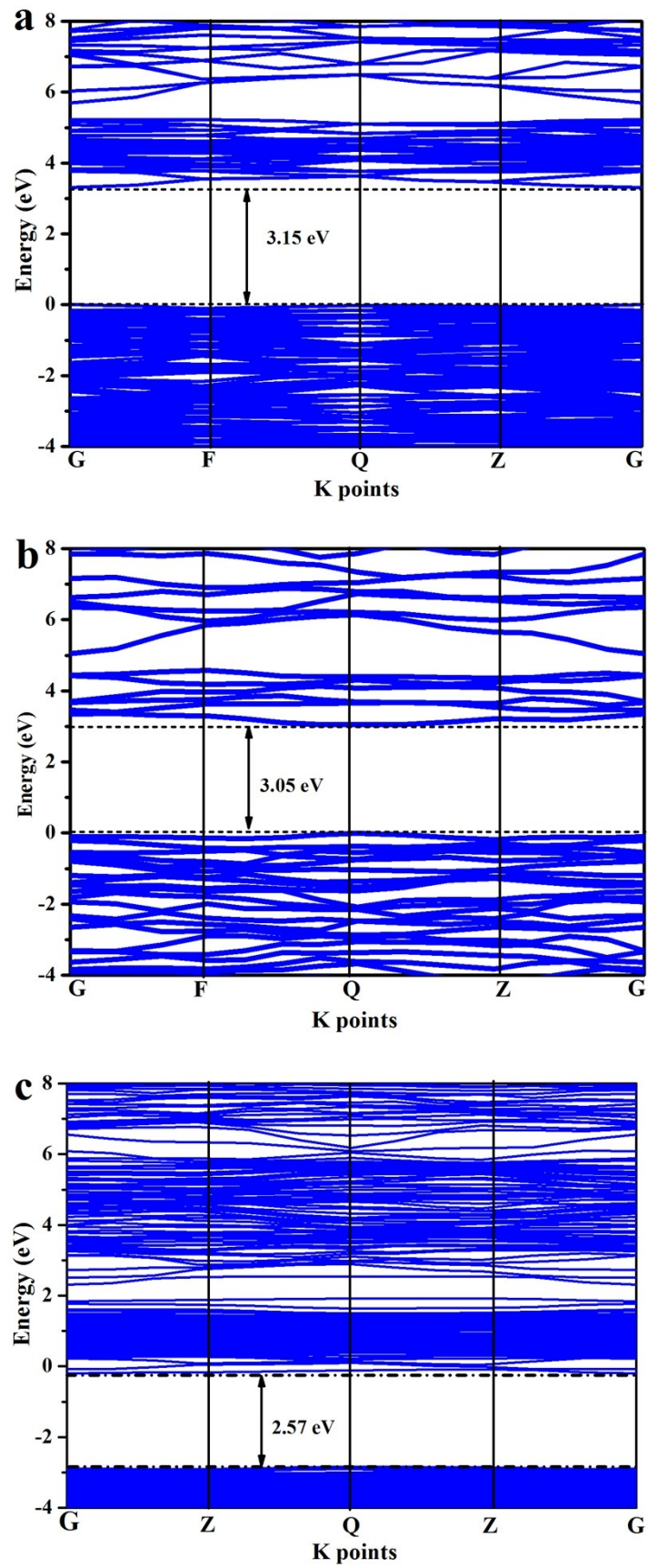


Fig. S2 The band structure model diagram of ZWO (a), 0.6L-ZWO (b), and 0.6L-ZWO-OVs (c)

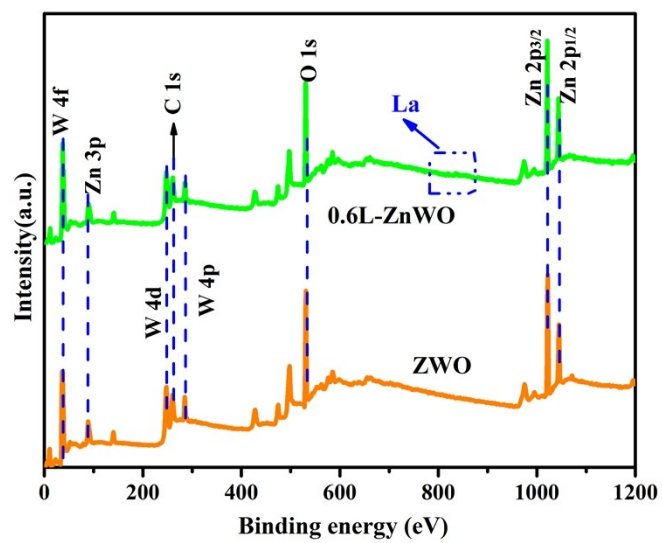


Fig. S3 XPS survey spectra of ZWO and 0.6L- ZWO samples

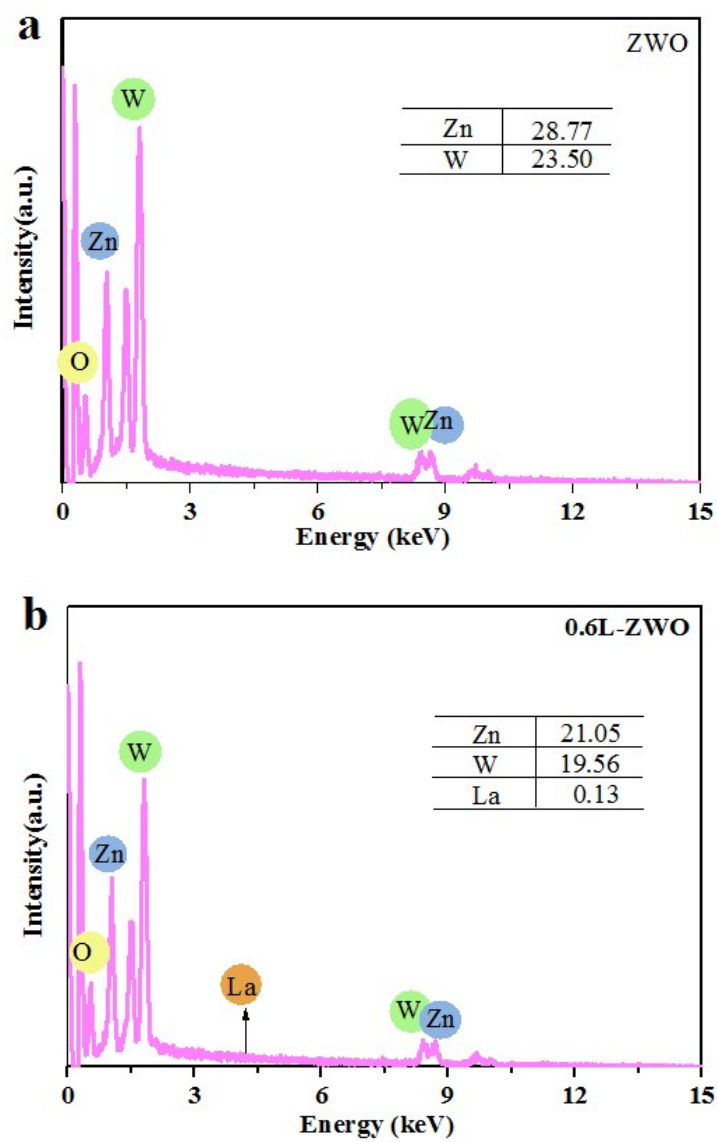


Fig. S4 EDS spectrum of ZWO (a) and 0.6L-ZWO (b) samples

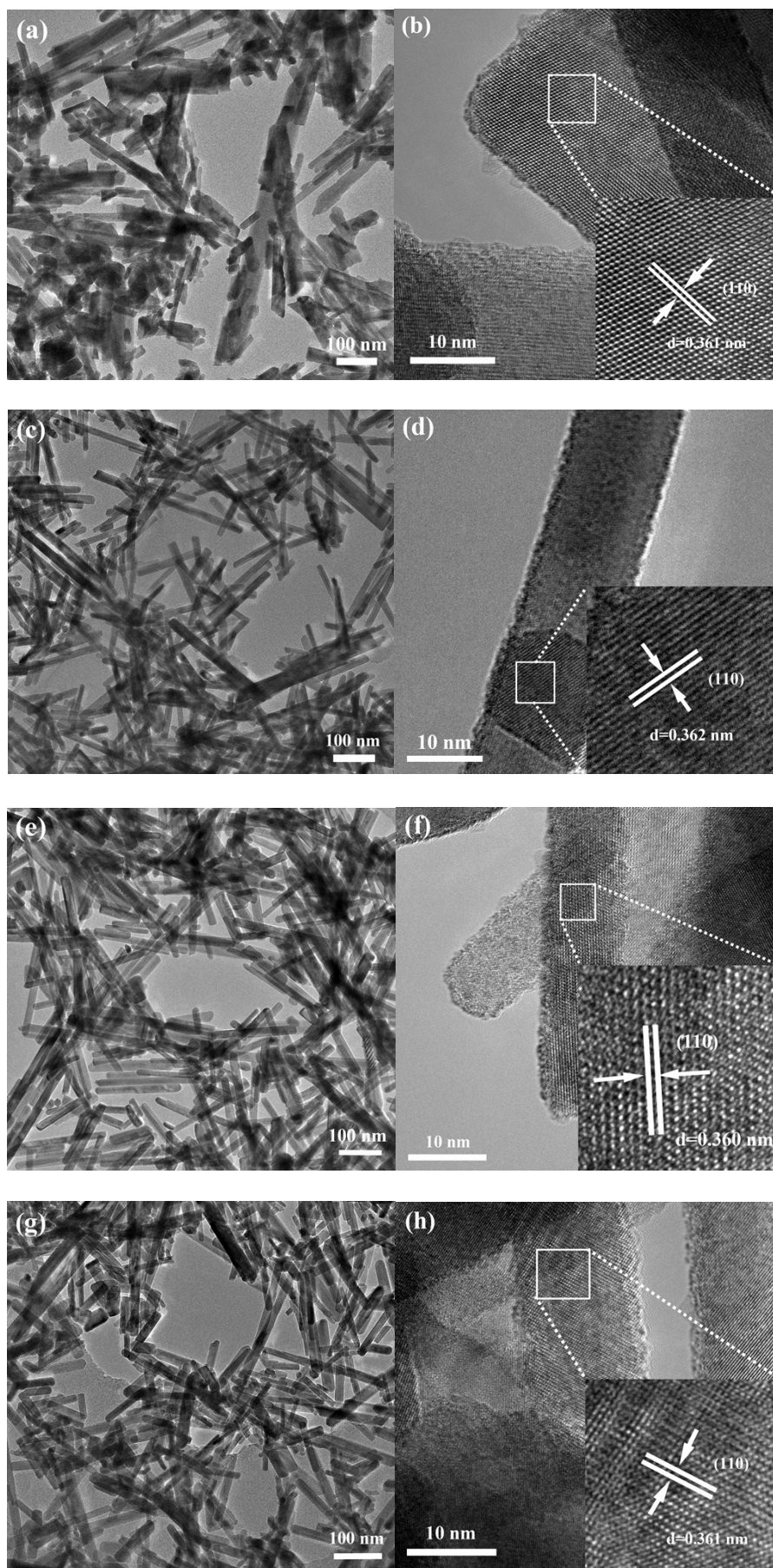


Fig. S5 TEM images of ZWO (a,b), 0.4L-ZWO (c,d), 0.8L-ZWO (e,f), and 1.2L-ZWO (g,h)

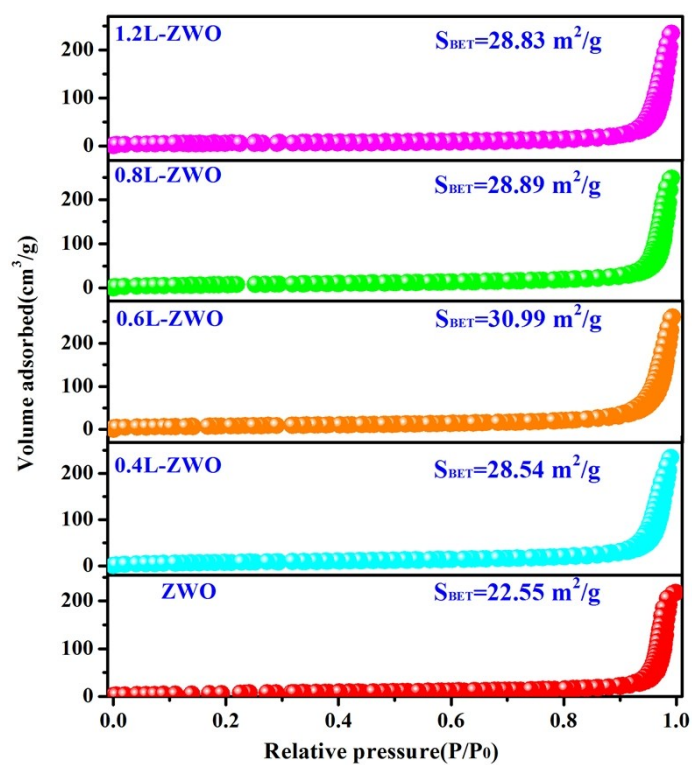


Fig. S6 Nitrogen adsorption-desorption isotherms of all as-prepared samples

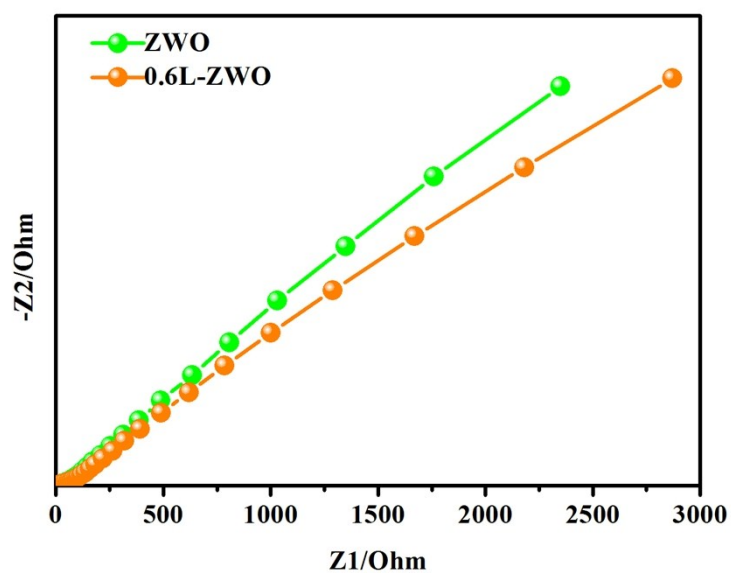


Fig. S7 EIS Nyquist plots of ZWO and 0.6L-ZWO

As we known, the photocatalytic performance of the photocatalysts is correlated to various factors including the light source, the type of photocatalyst, experimental environment, and initial concentration of gas. These factors lead to the quite differently photocatalytic efficiency. Therefore, the comparison based on photocatalytic activity of several selected photocatalysts, light source, and light intensity is given in Table 1.

Table 1 The description of selected photocatalysts for NO_x removal

Photocatalyst	Light source	Light intensity	NO _x removal rate	Reference
g-C ₃ N ₄ /TiO ₂	15W tungsten halogen lamp	100 mW/cm ²	30.2 %	1
g-C ₃ N ₄	15W tungsten halogen lamp	100 mW/cm ²	33 %	2
C doped (BiO) ₂ CO ₃	300 W tungsten halogen lamp	-	46.1 %	3
Zn-S-TiO ₂	mercury UV lamp	200 mW/cm ²	30 %	4
TiO ₂	mercury UV lamp	100 mW/cm ²	32%	5
(BiO) ₂ CO ₃	150 W tungsten halogen lamp	-	40 %	6
La ³⁺ -ZnWO ₄	300 W Xenon lamp	80 mW/cm ²	46 %	Our work

It can be seen from the Table 1, the photocatalytic performance of the photocatalysts is greatly affected by various factors including the light source, the type of photocatalyst, and light intensity of the light source. Compared with other photocatalysts in this table, the NO_x removal efficiency of the as-prepared La³⁺-ZnWO₄ photocatalyst is higher in this work.

Reference

1 I. Papailias, N. Todorova, T. Giannakopoulou, J. Yu, D. Dimotikali and C. Trapalis,

Photocatalytic activity of modified g-C₃N₄/TiO₂ nanocomposites for NO_x removal, *Catal. Today*, 2017, **280**, 37-44.

2 I. Papailias, N. Todorova, T. Giannakopoulou, S. Karapati, N. Boukos, D. Dimotikali and C. Trapalis, Enhanced NO₂ abatement by alkaline-earth modified g-C₃N₄ nanocomposites for efficient air purification, *Appl. Surf. Sci.*, 2018, **430**, 225-233.

3 F. Dong, Y. Sun, W. K. Ho, Z. Wu, Controlled synthesis, growth mechanism and highly efficient solar photocatalysis of nitrogen-doped bismuth subcarbonate hierarchical nanosheets architectures, *Dalton Trans*, 2012, **41**, 8270-84.

4 D. Papoulis, K. Somalakidi, N. Todorova, C. Trapalis, D. Panagiotaras, D. Sygkridou, E. Stathatos, E. Gianni, A. Mavrikos and S. Komarneni, Sepiolite/TiO₂ and metal ion modified sepiolite/TiO₂ nanocomposites: synthesis, characterization and photocatalytic activity in abatement of NO_x gases, *Appl. Clay. Sci.*, 2019, **179**, 105156.

5 M. Xu, Y. Bao, K. Wu, T. Xia, H. L. Clack, H. Shi and V. Li, Influence of TiO₂ incorporation methods on NO_x abatement in Engineered Cementitious Composites, *Constr. Build. Mater.*, 2019, **221**, 375-383.

6 F. Dong, J. Bian, Y. Sun, T. Xiong and W. Zhang, The rapid synthesis of photocatalytic (BiO)₂CO₃ single-crystal nanosheets via an eco-friendly approach, *CrystEngComm*, 2014, **16**, 3592-3604.